# Development and Characterization of Folic acid Conjugated Paclitaxel Bearing Microspheres for the Effective Treatment of Colorectal Cancer

Shrutimayee Patra, Sunny Rathee, Amit Sahu, Sarjana Raikwar, Umesh K. Patil, Sanjay K. Jain\*

Pharmaceutics Research Projects Laboratory, Department of Pharmaceutical Sciences, Dr. Harisingh Gour Vishwavidyalaya, (A Central University), Sagar (M.P.), INDIA - 470003 Corresponding author email: drskjainin@gmail.com

(Received on 12/10/2022; Accepted on 16/11/2022)

# **Abstract**

The purpose of this study was to develop folic acid conjugated paclitaxel loaded microspheres for the treatment of colorectal cancer. To achieve this, several key chemical compounds were synthesized: a valine-paclitaxel conjugate, which could potentially enhance the properties of paclitaxel; folic acid-N-hydroxysuccinimide (FA-NHS), a reagent commonly used to activate carboxyl groups, likely facilitating the conjugation of folic acid; and the folic acid-paclitaxel (FA-PTX) conjugate, which aimed to enable targeted delivery of paclitaxel to cancer cells. The ionic gelation method was employed for the preparation of microspheres using chitosan, acetic acidand sodium tripolyphosphate (TPP) solution. The prepared microspheres were assessed for various parameters such as surface morphology, vesicle size, zeta potential, percentage entrapment efficiency (%EE), and *in vitro* drug release. The results of SEM depicted that the morphology of folic acid conjugated paclitaxel loaded microspheres were found to be 6.9±2.41 µm and 0.247, respectively. The Zeta Potential of folic acid conjugated paclitaxel loaded microspheres was found to be 7.24±0.34 mV. The %EE of folic acid conjugated paclitaxel loaded microspheres was found to be 85.00±0.5 %. The drug release from the folic acid conjugated paclitaxel loaded microspheresafter 72 hrs was found to be 77.2±1.9% and 60.3±2.2%at pH 6.8 and pH 7.4, respectively. These results showed that folic acid conjugated paclitaxel loaded microspheres could be a potential approach for the effective treatment of colorectal cancer.

Keywords: Paclitaxel (PTX); Microspheres; Folic Acid (FA); Chitosan; fmoc-Valine

# Introduction

fatalities occurring in individuals newly diagnosed with the disease at age 65 or older in 2014 (Siegel et al., 2020). The treatment of colorectal cancer remains a formidable task, with limited options beyond palliative care (Biller & Schrag, 2021; Hashiguchi et al., 2020). The conventional approach to colorectal cancer treatment involves systemic chemotherapy, resulting in a median survival time of less than 12 months for patients (Kim & Kim, 2021). Given the locoregional nature of colorectal cancer dissemination, exploring local treatment options has become imperative—(Moretto et al., 2020).

In the pursuit of suitable carriers for the locoregional delivery of anticancer drugs, researchers have turned to micro- and nanoparticles to achieve encouraging results (Rossi et al., 2021). Microspheres have demonstrated the ability to deliver drugs locally, increasing their anticancer efficacy while reducing side effects. Microspheres also provide a means to overcome challenges associated with systemic chemotherapy, such as renal clearance and degradation by serum nucleases (Fan et al., 2016). The size and shape of these carriers significantly influence their circulation times and their ability to navigate biological barriers.

Tsai et al., 2007 study emphasizes the pivotal role of drug carriers in the antitumor activity of intraperitoneal chemotherapy, with microparticles demonstrating a distinct advantage, including longer residence times, superior peritoneal targeting, and extended survival, compared to nanoparticle formulations. This compelling evidence has led to the adoption of microspheres as a preferred modality for chemotherapy delivery. Among the critical structural attributes of a drug delivery system, the porosity and size of microspheres play a pivotal role in shaping drug release kinetics and degradation behaviour (Tsai et al., 2007).

Paclitaxel (PTX), a natural alkaloid derived from the bark of *Taxus brevifolia*, has emerged as a cornerstone in the treatment of various tumours (Sharifi-Rad et al., 2021). Recent research indicates that low-dose PTX holds promise as a treatment for certain cancers, offering minimal side effects. PTX achieves its therapeutic effects by stabilizing polymerized microtubules, enhancing microtubule assembly, arresting the cell cycle, and inducing apoptosis (Lv et al., 2017). Despite its efficacy, high-dose PTX is associated with significant side effects, including peripheral neuropathy and anaphylactic hypersensitivity reactions (Abu Samaan et al., 2019). In response to these challenges, low-dose metronomic

PTX chemotherapy has gained prominence as an alternative with high efficacy, low toxicity, and reduced drug resistance in clinical settings.

However, it is important to acknowledge that PTX, like other cytotoxic agents, may not discriminate between tumour and healthy cells, potentially leading to severe toxicity at therapeutic doses (Nars & Kaneno, 2013). Consequently, combination therapy with different drugs has become a critical strategy in the treatment of cancers, aiming to enhance antitumor efficacy while minimizing drug resistance. Several combination remedies incorporating natural herbs have been proposed to reduce the required drug dosage.

In light of these challenges and opportunities, this research paper explores the utilization of microspheres as carriers for the local delivery of low-dose PTX in the treatment of colorectal cancer. Our study delves into the impact of microsphere size, shape, and porosity on drug release kinetics and degradation behaviour. Additionally, it is investigated the potential advantages of combining low-dose PTX with natural herb-containing combination remedies to enhance anticancer efficacy while reducing toxicity. This research aims to contribute to the development of more effective and targeted therapies for colorectal cancer, offering new hope for patients facing this formidable disease.

# Materials and method

### **Materials**

Paclitaxel was provided as a gift sample by Neon Laboratories, Mumbai. N-Hydroxysuccinimide (NHS) was procured from Himedia, while EDC, fmoc valine, and Anhydrous Magnesium Sulphate were purchased from Sigma-Aldrich (Mumbai, India). DMAP was acquired from Qualigens, India, and the dialysis membrane, featuring a 12 KDa molecular weight cutoff, was obtained from Himedia Lab Pvt. Ltd.

# Methodology

# Conjugation of Paclitaxel (PTX) with Folic Acid (FA)

The preparation of FA-PTX followed the method outlined by Wang et al., 2015 which comprises three distinct steps (Wang et al., 2015).

# Step 1: Synthesis of Valine-PTX Conjugate

To synthesize Valine-PTX, 85.3 mg of paclitaxel (PTX) and an excess amount of Fmoc-Valine (37.5 mg) were dissolved in dichloromethane (DCM). Equimolar amounts of DMAP (4-dimethylaminopyridine) were added, and the reaction was allowed to proceed at 0°C for 1 hour with continuous stirring. Subsequently, 1.9 mg of EDC was added, and the reaction continued at 0°C for an additional 1 hour. Afterward, the mixture was reacted for an additional 8 hours at room temperature. To separate the organic and aqueous phases, a 0.05N HCl solution was added, and dichloromethane (DCM) was used to extract the aqueous phase. The DCM-extracted solution was combined with the organic phase, and the

concentrated solution was obtained by absorption using anhydrous magnesium sulphate (MgSO $_4$ ). Additional DCM was added to the concentrated solution. Valine-PTX was finally obtained by removing the solvent and precipitating the compound in n-hexane.

**Figure 1.** Schematic representation of steps involved in synthesis V-PTX

# Step 2: Synthesis of FA-NHS

The synthesis of FA-NHS involved dissolving 100 mg of folic acid in 2 ml of dimethyl sulfoxide (DMSO). To this solution, 26.07 mg of N-hydroxysuccinimide (NHS) and 43.32 mg of 1-ethyl-3-(3-dimethylaminopropyl)carbodiimide (EDC) were added. The reaction was allowed to proceed at room temperature for 40 hours in a dark place. After completion of the reaction, FA-NHS was obtained by filtering the solution and subsequently drying it under vacuum.

**Figure 2.** Schematic representation of steps involved in synthesis of NHS-FA

### Step 3: Synthesis of FA-PTX

The synthesis of FA-PTX was achieved by using V-PTX and FA-NHS, which were synthesized in the previous steps. Both V-PTX and FA-NHS were separately dissolved in dimethyl sulfoxide (DMSO). These solutions were then mixed and allowed to react for 48 hours at room temperature. Following

the reaction, the mixture was purified by dialysis using a dialysis membrane for 48 hours. This process is helped to remove excess FA-NHS and other impurities from the solution. The final product, FA-PTX, was obtained by subjecting the purified solution to lyophilization using a lyophilizer (Xin et al., 2010).

Figure 3. Schematic representation of steps involved in synthesis of FA-PTX

### Preparation of microspheres

A chitosan solution was prepared by adding the specified amount of chitosan to a 1% v/v acetic acid solution. The mixture was stirred for one hour. Separately, paclitaxel was dissolved in absolute ethanol and then added to the previously prepared chitosan solution. The resulting mixture was stirred for 15 minutes, leading to the formation of paclitaxel (PTX) dispersion within the chitosan solution. To produce chitosan microspheres, 20 ml of a sodium tripolyphosphate (TPP) solution was placed in a beaker, and 10 ml of the chitosan solution was added using a glass syringe fitted with an 18 G

needle. Stirring was conducted for 15 minutes to obtain the microspheres in a wet state. These wet microspheres were separated through filtration using Whatman No.1 Qualitative filter paper. To further treat the microspheres, 10 ml of acetone was introduced to the particles remaining on the filter paper. The microspheres were subsequently transferred to a beaker containing 20 ml of acetone and mixed for a few minutes. The drying process was performed by placing the particles in a petri dish at room temperature for 18 hours, resulting in the formation of chitosan microspheres (Ismail et al., 2015) (Figure 4).

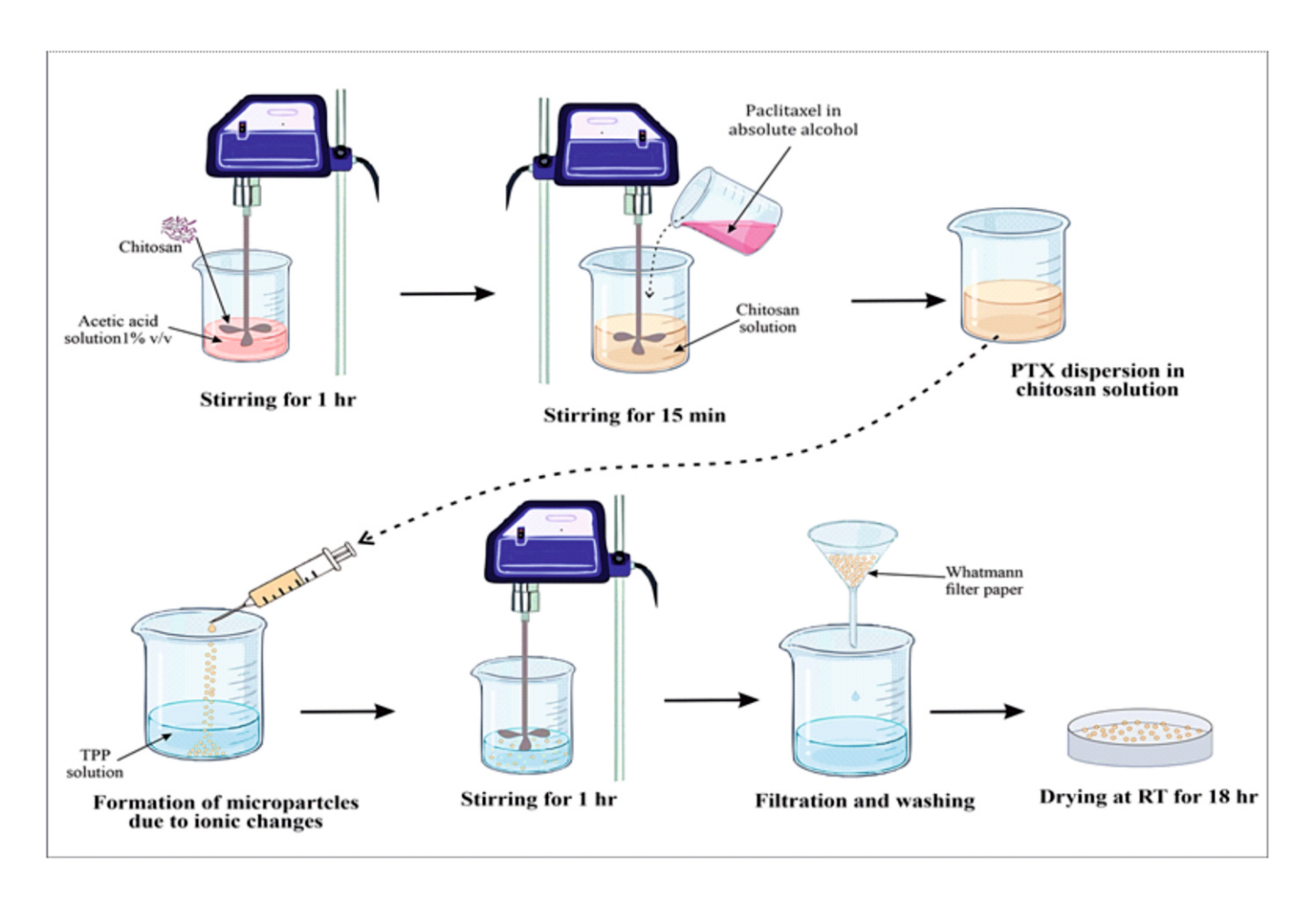


Figure 4. Diagrammatic representation of method of preparation of microsphere by ionic gelation method

# **Optimization**

The preparation and properties of microspheres are influenced by a range of variables, including both process variables and formulation variables. These variables were systematically optimized and studied during the research. Process variables encompass factors such as stirring speed and stirring time, while formulation variables include polymer concentration and the concentration of the cross-linking agent (TPP). The optimization process considered key factors such as particle size and entrapment efficiency as criteria for assessing the microspheres properties (Gohel & Amin, 1998).

### 1. Optimization of formulation variables

- ✓ Optimization of polymer concentration
- ✓ Optimization of TPP concentration

# 2. Optimization of process variables

- ✓ Optimization of stirring speed
- ✓ Optimization of stirring time

### **Optimization of formulation variables**

Optimization of polymer Concentration

To optimize polymer concentration, microspheres were prepared using different polymer concentrations, ranging from 50, 75, 100, to 125 mg (as shown in **Table 3** and **Figure 9**). The optimized polymer concentration was determined to be 50 mg based on the evaluation of average particle size and entrapment efficiency. This optimization process aimed to identify the most suitable polymer concentration for achieving the desired microsphere properties.

# Optimization of TPP concentration

For the optimization of the concentration of TPP, microsphere formulations were prepared using various concentrations of TPP in the aqueous medium, while keeping other formulation variables constant. The influence of TPP concentration on particle size and entrapment efficiency was assessed, and the results are presented in **Table 4** and **Figure 10**. This investigation aimed to determine the ideal concentration of TPP that would yield the desired outcomes for particle size and entrapment efficiency in the microspheres.

### Optimization of process variables

Indeed, various process variables, including stirring speed and stirring time, play a significant role in the formulation of microspheres. Therefore, it is essential to optimize these parameters to achieve the desired properties and characteristics in the formulation. By systematically adjusting and optimizing these process variables, researchers can fine-tune the microsphere preparation process to meet

specific objectives and criteria.

### Optimization of stirring speed

The stirring speed of the magnetic stirrer was systematically varied, ranging from 500 to 2000 rpm, while maintaining the other formulation parameters constant. The resulting microspheres were evaluated for their particle size and entrapment efficiency, and the findings are detailed in **Table 5** and **Figure 11**. This investigation allowed for the assessment of the impact of stirring speed on the microsphere properties.

# Optimization of stirring time

In the optimization process for stirring time, with all other variables held constant, the microspheres were prepared with varying stirring time periods, specifically 60, 90, 120, and 150 minutes. Subsequently, the particle size and entrapment efficiency of these microspheres were assessed, and the results are presented in **Table 6** and **Figure 12**. This investigation allowed for the evaluation of the impact of stirring time on the properties of the microspheres and provided valuable insights for optimization.

# Characterization

### Particle size determination

The size and size distribution of the microspheres were assessed using Dynamic Light Scattering (DLS) with Photon Correlation Spectroscopy (PCS), specifically employing NanoPlus-2 (Version 5.01, Micromeritics Instrument Corporation, Particulate Systems, Norcross, GA, USA). To determine the average particle size and polydispersity index of the microspheres, the samples were dispersed in water. The particle size distribution was represented by the average size (diameter) and the variance (polydispersity) of the Gaussian distribution function in logarithmic axis mode, as illustrated in **Figure 13**. This analysis provided valuable insights into the size and distribution of the microspheres (Verma et al., 2021).

# Surface charge determination

The surface charge of microspheres was determined by measurement of zeta potential. The zeta potential of the microspheres was determined using NanoPlus-2 (Version 5.01, Micromeritics Instrument Corporation, Particulate Systems, Norcross, GA, USA). The formulation of microspheres was found to be positively charged.

### Scanning Electron Microscopy (SEM)

The particle morphology of the microspheres was analyzed using Scanning Electron Microscopy (SEM). SEM analysis was conducted using the NOVA NANOSEM 450 instrument. To prepare the samples for SEM, the microspheres were lightly sprayed onto an adhesive carbon tape, which was affixed to an aluminum stub. These stubs were subsequently coated with a layer of gold to the desired thickness. The samples were then examined under the scanning electron microscope, operating at a voltage of 20 kV. Photomicrographs were captured at varying magnifications, and these images are presented in **Figure 15**. SEM analysis allowed for the visualization and characterization of the

microsphere's surface and structure (Panda & Jain, 2023).

# **Entrapment efficiency**

The Paclitaxel content within the microspheres was quantified using a method outlined by Dozie-Nwachukwu et al., 2017 (Dozie-Nwachukwu et al., 2017). Initially, 10 mg of Paclitaxel-loaded microspheres were finely ground using a mortar and pestle. The resulting powder was then suspended in a 10 ml phosphate buffer pH of 7.4. To ensure even dispersion, the mixture underwent a 10-minute sonication process. Subsequently, it was left to stand at room temperature for a period of 24 hours. Following incubation, centrifugation was employed, separating the microsphere particles from the supernatant, which contained the released Paclitaxel. The Paclitaxel concentration was then determined by measuring absorbance at 230 nm to known concentrations of Paclitaxel. All sample analyses were performed in duplicate to ensure the accuracy and reliability of the results. This method proved essential for the precise quantification of Paclitaxel content in the microspheres, offering valuable insights into drug-loading efficiency and release characteristics.

 $\% EE = \left(TD - \frac{FD}{TD}\right) * 100$ 

TD = Total drug, FD = Free drug

### In-vitro drug release study

FA-PTX microsphere formulation's in-vitro drug release studies were conducted using a dialysis bag method with a molecular cut-off point of 3,500 at pH 6.8 and pH 7.4, as reported by Wang et al. 2016(Wang et al., 2016). The FA-PTX microsphere suspension was placed in a dialysis bag and immersed in a beaker containing 100 ml of PBS pH 7.4/PB pH 6.8. The beaker was kept on a magnetic stirrer (50 rpm) at  $37\pm0.5^{\circ}\text{C}$  throughout the study. At definite time intervals, the samples were withdrawn and replaced with the same volume of respective fresh PBS pH 7.4/PB pH 6.8 to maintain constant volume. The withdrawn samples were analysed for drug content using a UV spectrophotometer at 230 nm after filtering with Whatman No. 41 filter paper.

# Statistical analysis

All experiments were performed in triplicate and data were expressed as mean  $\pm$  SD. GraphPad Prism 7.0 software was used to perform the statistical analyses. P-value <0.001 was considered statistically significant.

# **Results and Discussion**

# Characterization of Conjugate

Characterization of NHS-FA Conjugate

The interpretation of the FTIR and H¹ NMR spectra for the NHS-FA conjugate in the first step of the conjugation process provides valuable insights into its chemical composition. In the FTIR spectrum, the presence of functional groups is evident. The peaks in the 3520-3200 cm⁻¹ range suggest N-H stretching, potentially originating from the aromatic amine groups in the conjugate. The 3000-2500 cm⁻¹ range indicates aliphatic C-H stretching, likely associated with the

succinimide portion. The appearance of peaks at 1474 cm<sup>-1</sup> (C-H bending) and 1330 cm<sup>-1</sup> (CH bending) suggests carbonhydrogen bonds, possibly from aliphatic moieties. Peaks at 1660 cm<sup>-1</sup> (N=O bend) and 1697 cm<sup>-1</sup> (C=O bend) imply the presence of nitroso and carbonyl groups, which could correspond to the NHS and folic acid components, respectively. In the H<sup>1</sup> NMR spectrum, chemical shifts in the range of 6.5-9 ppm indicate aromatic hydrogen atoms, which

align with the presence of an aromatic ring in folic acid. The chemical shift range of 2-3 ppm is associated with aliphatic hydrogens, likely originating from the succinimide group, and a peak at 11-12 ppm suggests hydroxyl protons from folic acid. Together, these spectra confirm the presence of key functional groups, indicating the successful formation of the NHS-FA conjugate in this initial conjugation step (Xin et al., 2010) (Figure 5, 6, and Table 1).

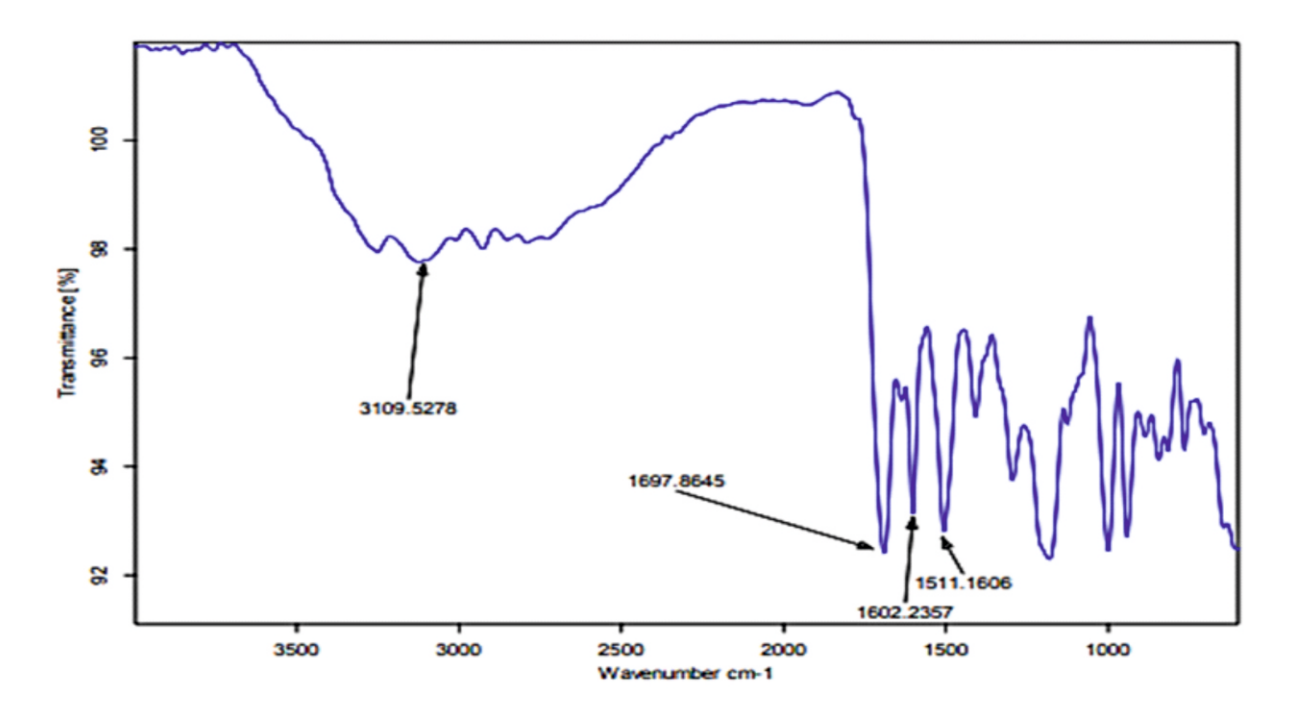


Figure 5. FTIR spectrum of NHS-FA Conjugate

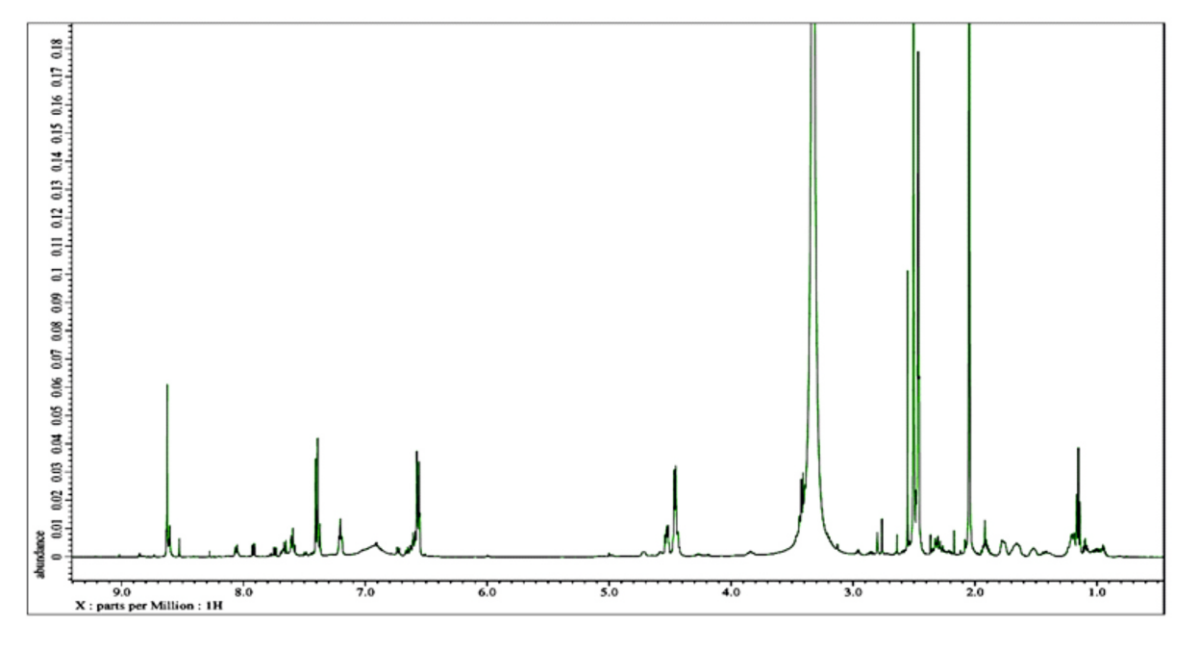


Figure 6. H<sup>1</sup> NMR of NHS-FA conjugate

**Table 1.** FTIR and H<sup>1</sup> NMR Peaks of NHS-FA conjugate

FTIR Spect	roscopy	H <sup>1</sup> N	MR
Wave number(cm <sup>-1</sup> )	Functional groups	Chemical shift (ppm)	Hydrogen group
3520-3200	N-H stretching	6.5-9	Aromatic-H
3000-2500	C-H stretching	2-3	H-Succinimide
1474	C-H bending	11-12	О-Н
1330	CH bending		
1660	N=O bend		
1697	C=O bend		

# Characterization of FA-PTX Conjugate

The interpretation of the FTIR and H¹ NMR spectra for the FA-PTX conjugate in the second and third steps of the conjugation process sheds light on its chemical composition. In the FTIR spectrum, a peak at 3117.86 cm¹ indicates aromatic stretching, likely originating from the phenyl ring within folic acid (FA) or another aromatic group present in the conjugate. The appearance of a peak at 1684.94 cm¹ suggests the presence of carbon-carbon double bonds (C=C), which can be attributed to the PTX (paclitaxel) component. The N-H bending peak at 1599.46 cm¹ signifies the presence of amine (N-H) functional groups, potentially from FA or other elements within the conjugate. Peaks at 1245.68 cm¹ (C-O

Stretching), 1114.13 cm<sup>-1</sup> (C-N Stretching), and 694.56 cm<sup>-1</sup> (Aromatic out of plane bending) further validate the existence of various chemical groups within the conjugate. In the H<sup>1</sup>NMR spectrum, chemical shifts in the ranges of 0.5-4.0 ppm (R-NH), 0.5-5.0 ppm (R-OH), 0.7-1.3 ppm (R-CH<sub>3</sub>), and 1.2-1.4 ppm (R-CH<sub>2</sub>-R) suggest the presence of amine, hydroxyl, methyl, and methylene groups, respectively, originating from different parts of the conjugate. Chemical shifts in the range of 2.3-2.7 ppm (C<sub>6</sub>H<sub>5</sub>-CH-R) and 4.5-6.5 ppm (R-C=C-H) indicate the presence of protons adjacent to aromatic rings and double bonds, respectively, supporting the composition of the FA-PTX conjugate in these subsequent steps of the conjugation process (Xin et al., 2010) (**Figure 7, 8, and Table 2**).

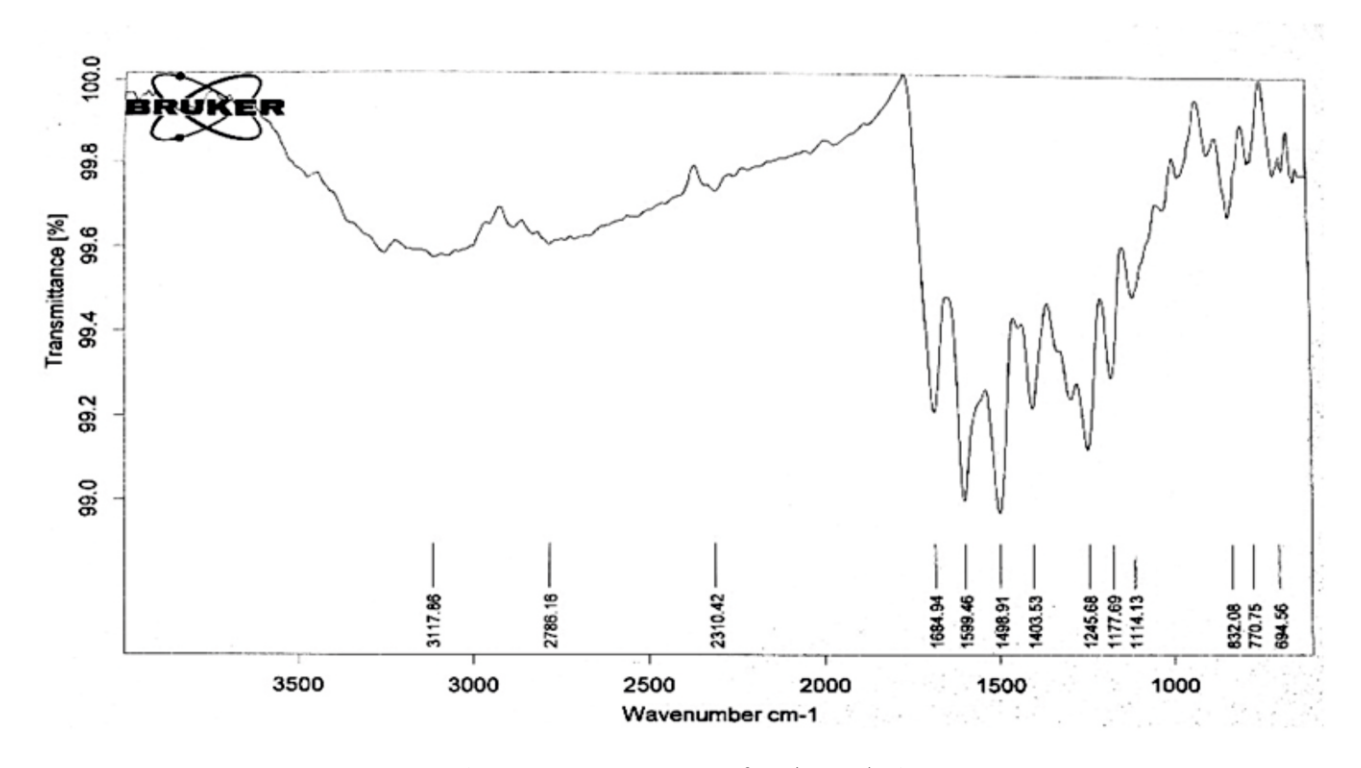


Figure 7. FTIR spectrum of conjugated FA-PTX

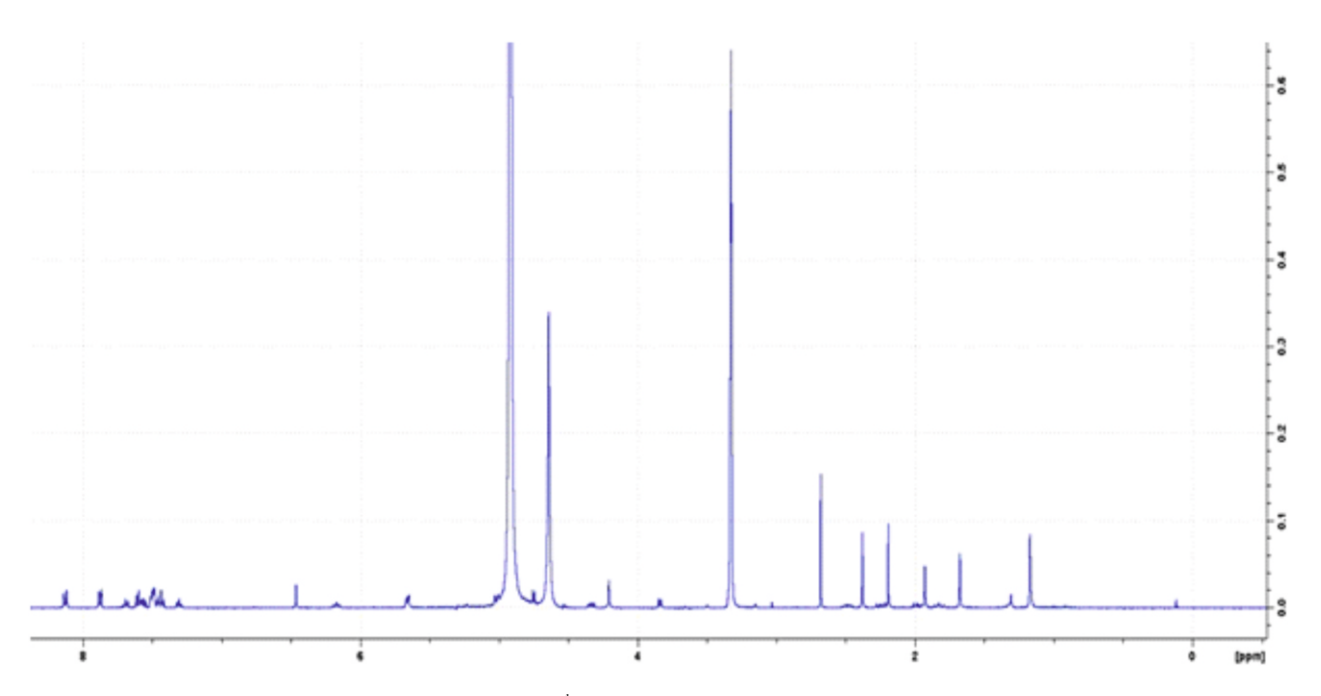


Figure 8. H<sup>1</sup>NMR of conjugated FA-PTX

**Table 2.** FTIR and H<sup>1</sup> NMR Peaks of FA-PTX conjugate

FTIR Sp	ectroscopy	$H^1 N$	MR
Wave number (cm <sup>-1</sup> )	Functional groups	Chemical shift (ppm)	Hydrogen group
3117.86	Aromatic stretching	0.5-4.0	R-NH
1684.94	C=C Stretching	0.5-5.0	R-OH
1599.46	N-H Bending	0.7-1.3	R-CH <sub>3</sub>
1245.68	C-O Stretching	1.2-1.4	R-CH <sub>2</sub> -R
1114.13	C-N Stretching	2.3-2.7	C <sub>6</sub> H <sub>5</sub> -CH-R
694.56	Aromatic out of plane bending	4.5-6.5	R-C=C-H

### **Optimization**

Theoptimization of various formulations was done involving various formulation variables including polymer concentration, Cross linking agent i.e. TPP concentration and process variables i.e. stirring time and stirring speed. Polymer concentration was optimized by varying concentration from 0.25%-1% (**Table 3**, **Figure 9**) and then optimize the TPP concentration from 1% to 2.5 % (**Table 4**, **Figure 10**), stirring time from 60-150 min (**Table 5**, **Figure 11**) and finally optimized stirring speed from 500-2000 rpm (**Table 6**, **Figure 12**).

Initially, the optimization process began with the assessment of Chitosan (a polymer) concentrations, and it was determined that a concentration of 0.50% w/v (referred to as P2) yielded favourable results based on particle size, Polydispersity Index (PDI), and the percentage of Paclitaxel (PTX) entrapment efficiency. At this concentration (0.50% w/v), chitosan provides a suitable balance between its role in forming the microspheres and the ability to encapsulate PTX efficiently.

Too low of a chitosan concentration may result in weak microspheres that cannot effectively entrap the drug, while too high of a concentration may lead to larger and less uniform particles. P2 appears to strike the right balance for microsphere formation and drug encapsulation. Subsequently, the concentration of Tripolyphosphate (TPP) was optimized. The effect of TPP concentration on particle size and PTX entrapment efficiency was evaluated. At a 1.5% concentration of TPP, a reduction in particle size and an increase in PTX entrapment efficiency were observed. The increased PTX entrapment efficiency at a higher TPP concentration can be attributed to the stronger interaction between TPP or the polymer matrix used for microsphere preparation. The tighter and more controlled structure formed at 1.5% TPP concentration may enable better encapsulation of PTX within the microspheres. Further increasing the TPP concentration resulted in an increase in particle size. This led to the formulation labelled as P2S2, representing the second stage of optimization.

The next step involved the fine-tuning of the formulation through the optimization of process variables like stirring speed, Stirring speed is a critical parameter in the formation of microspheres. At a speed of 1500 rpm, the turbulence and shear forces in the solution are likely optimized for the homogenization of the components. This can result in better mixing of the polymer, TPP, and the drug (PTX) and lead to more uniform particle sizes. This led to the formulation labelled as P2S2R3, representing the third stage of optimization.

Next step involved the fine-tuning of the formulation through the optimization of process variables like stirring time, extending the stirring time to 120 minutes allows for more thorough mixing and homogenization of the components in the formulation. This is particularly important for achieving a uniform distribution of the polymer (chitosan), TPP (cross-linking agent), and the drug (PTX) throughout the solution. Efficient mixing is crucial to ensure that each microsphere has a consistent composition and structure. This led to the formulation labelled as P2S2R3T3, representing the fourth stage of optimization.

Ultimately, the formulation denoted as P2S2R3T3 was identified as the optimal choice. In this optimized formulation, the average particle size was measured at 7  $\mu$ m, the PDI was found to be 0.239, and the PTX entrapment efficiency reached 85%. This rigorous scientific approach enabled the selection and fine-tuning of the most effective formulation, ensuring desirable characteristics for the efficient encapsulation of PTX.

Formulation code	Polymer Conc.(%w/v)	TPP Conc. (%w/v)	Stirring Speed(rpm)	Stirring Time (min)	Particle	PDI	% EE
P1	0.25%	1%	1000	60	7.0	0.441	83
P2	0.50%	1%	1000	60	8.4	0.272	85
Р3	0.75%	1%	1000	60	9.1	0.346	79
P4	1%	1%	1000	60	10	0.454	84

Table 3. Optimization of Polymer concentration

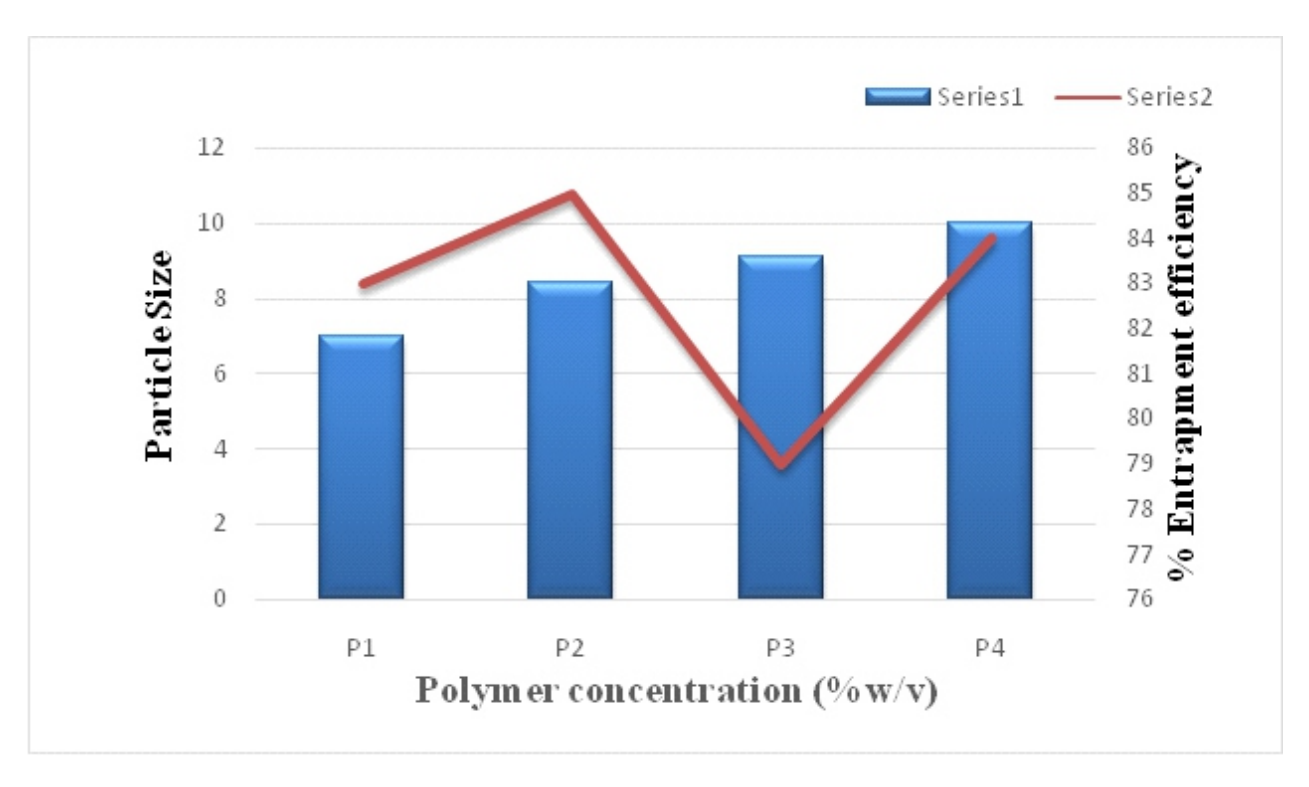


Figure 9. Effect of Polymer concentration on particle size and % entrapment efficiency

**Table 4.** Optimization of TPP concentration

Formulation code	Polymer Conc. (%w/v)	TPP Conc. (%w/v)	Stirring Speed(rpm)	Stirring Time (min)	Particle Size (µm)	PDI	% EE
P2S1	0.5%	1%	1000	60	8.1	0.423	77
P2S2	0.5%	1.5%	1000	60	6.9	0.247	82
P2S3	0.5%	2%	1000	60	7.1	0.326	80
P2S4	0.5%	2.5%	1000	60	7.4	0.330	79

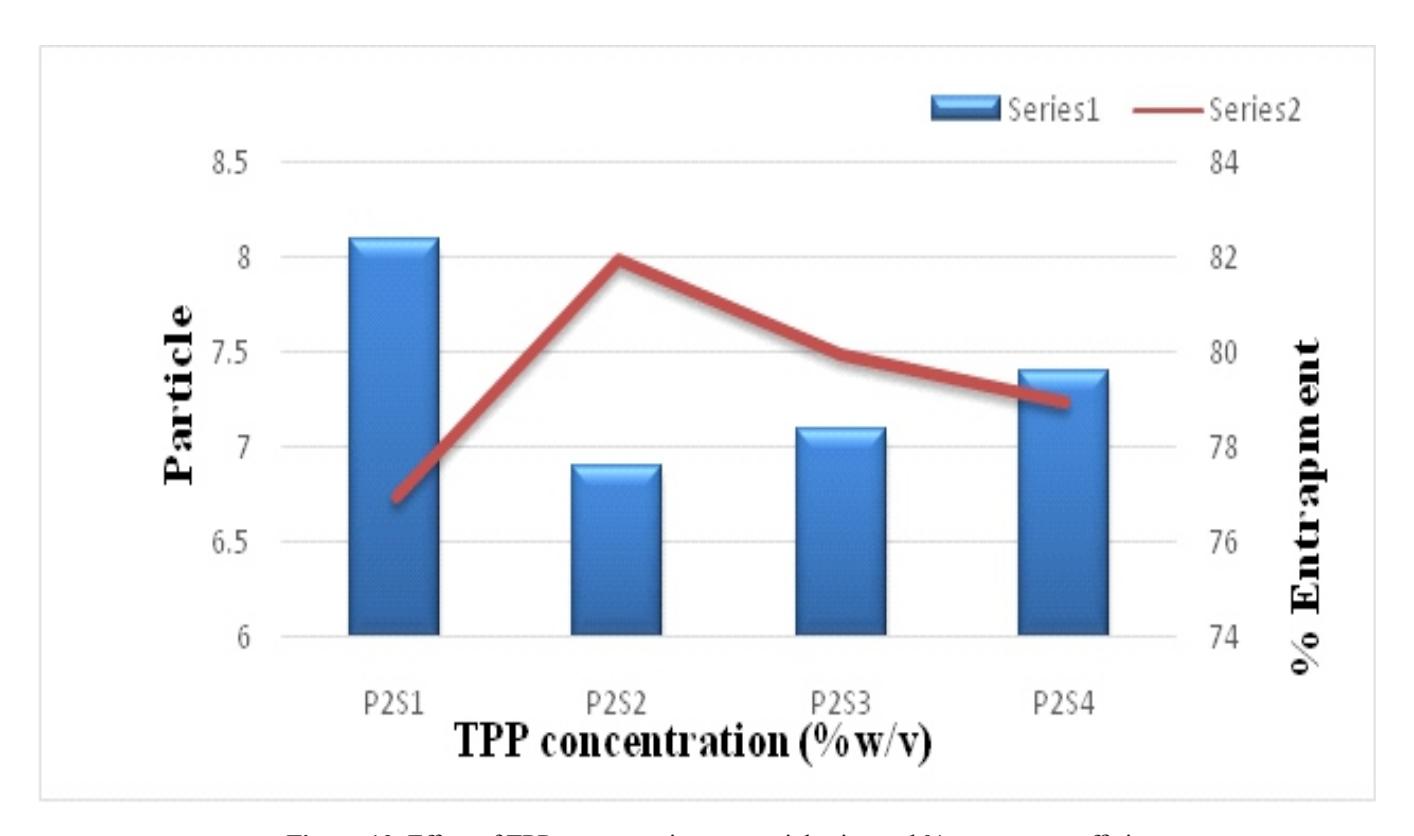


Figure 10. Effect of TPP concentration on particle size and % entrapment efficiency

Table 5. Optimization of Stirring speed

Formulation code	Polymer Conc. (%w/v)	TPP Conc.(%w/v)	Stirring Speed(rpm)	Stirring Time (min)	Particle Size (μm)	PDI	% EE
P2S2R1	0.5%	1.5%	500	60	10.1	0.523	84
P2S2R2	0.5%	1.5%	1000	60	9.8	0,399	81
P2S2R3	0.5%	1.5%	1500	60	6.7	0.201	85
P2S2R4	0.5%	1.5%	2000	60	6.3	0.603	84.4

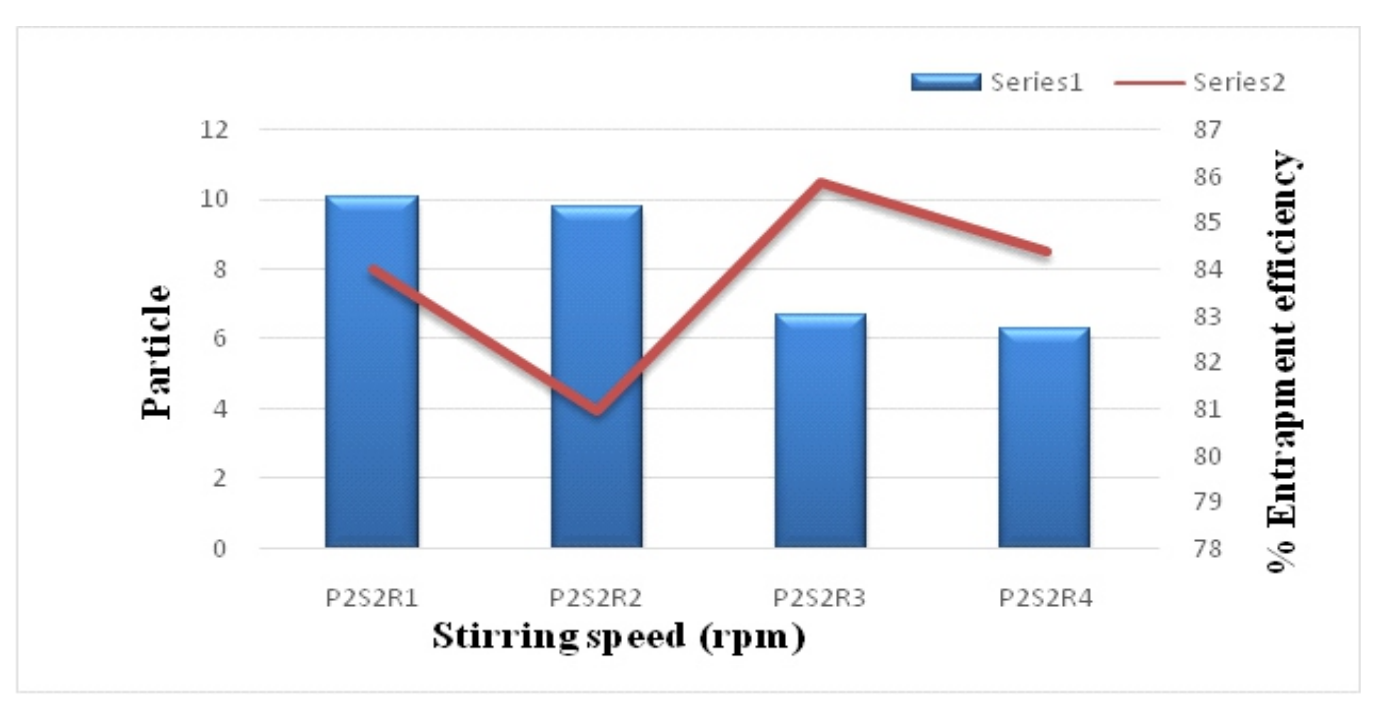


Figure 11. Effect of Stirring speed on particle size and % entrapment efficiency

**Table 6.** Optimization of Stirring time

Formulation code	Polymer Conc. (%w/v)	TPP Conc.(%w/v)	Stirring Speed(rpm)	Stirring Time (min)	Particle	PDI	% EE
P2S2R3T1	0.5%	1.5%	1500	60	8.8	0.445	84
P2S2R3T2	0.5%	1.5%	1500	90	8.7	0.325	80
P2S2R3T3	0.5%	1.5%	1500	120	6.9	0.247	85
P2S2R3T4	0.5%	1.5%	1500	150	5.8	0.321	78

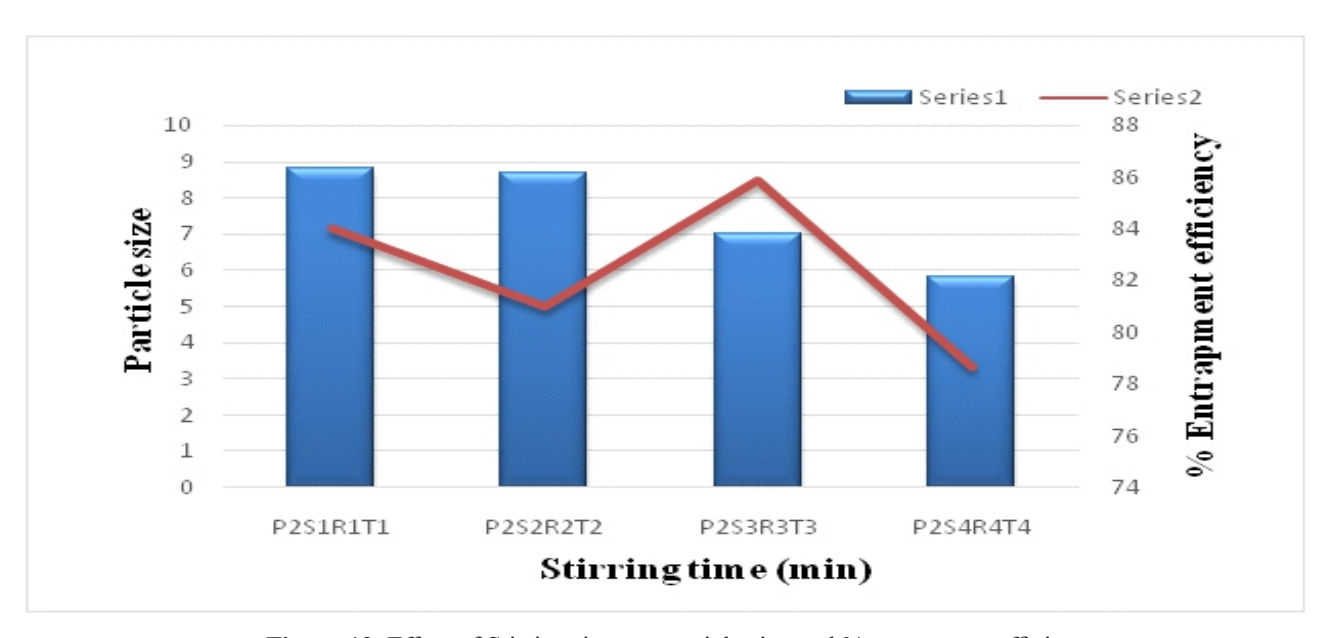


Figure 12. Effect of Stirring time on particle size and % entrapment efficiency

### Particle size and surface charge determination

The particle size and PDI of the conjugated microspheres were found to be  $6.9\pm2.41~\mu m$  and 0.247, respectively. The Zeta Potential of the conjugated microspheres was found to be  $7.24~\pm0.34~mV$ . The Zeta Potential is used to predict the stability of

a liposomal suspension (stability in terms of preventing aggregation). The vesicle size and zeta potential of conjugated microspheresare depicted in Figure 13, and 14, Table 7, and 8, respectively.

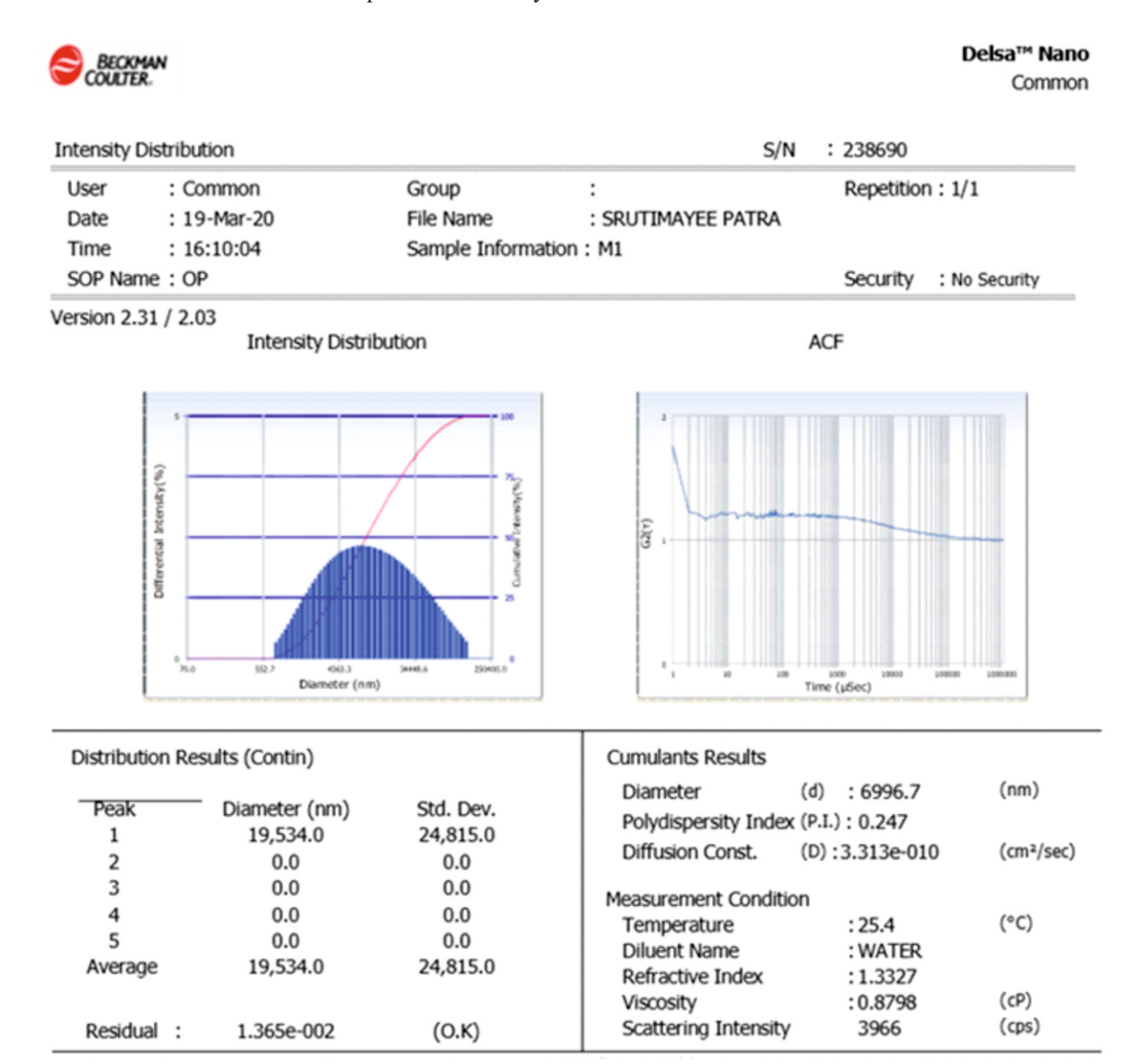


Figure 13. Report of Particle size and size distribution of microspheres

**Table 7.** Particle size and size distribution of microspheres

S. No	Formulation code	Size (μm)	PDI
1	P2S2R3S3	6.9± 2.41 μm	0.247

# Mobility Distribution

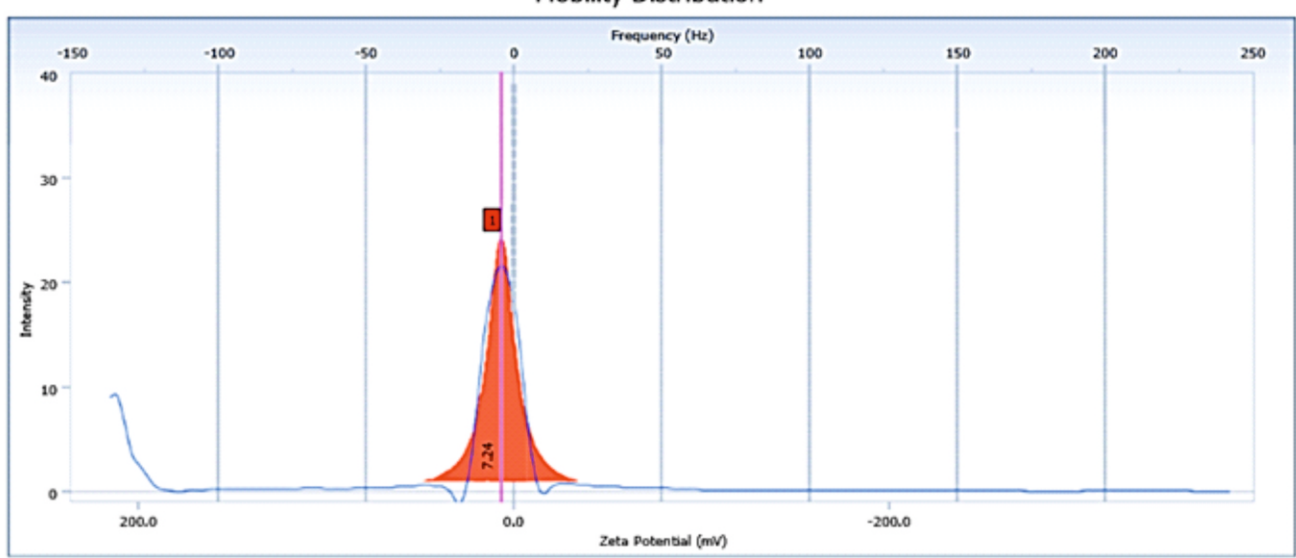


Figure 14. Report ofzeta potential analysis of microspheres

Table 8. Zeta potential analysis of microspheres

S. No	Formulation code	Zeta potential
1	P2S2R3S3	$7.24 \pm 0.34 \mathrm{mV}$

# Morphology

The morphology of the microspheres was investigated using Scanning Electron Microscopy (SEM) and images are shown

in **figure 15**, respectively. The result shows that the morphology of microspheres is generally spherical in shape with relatively smooth surface (Wang et al., 2016).

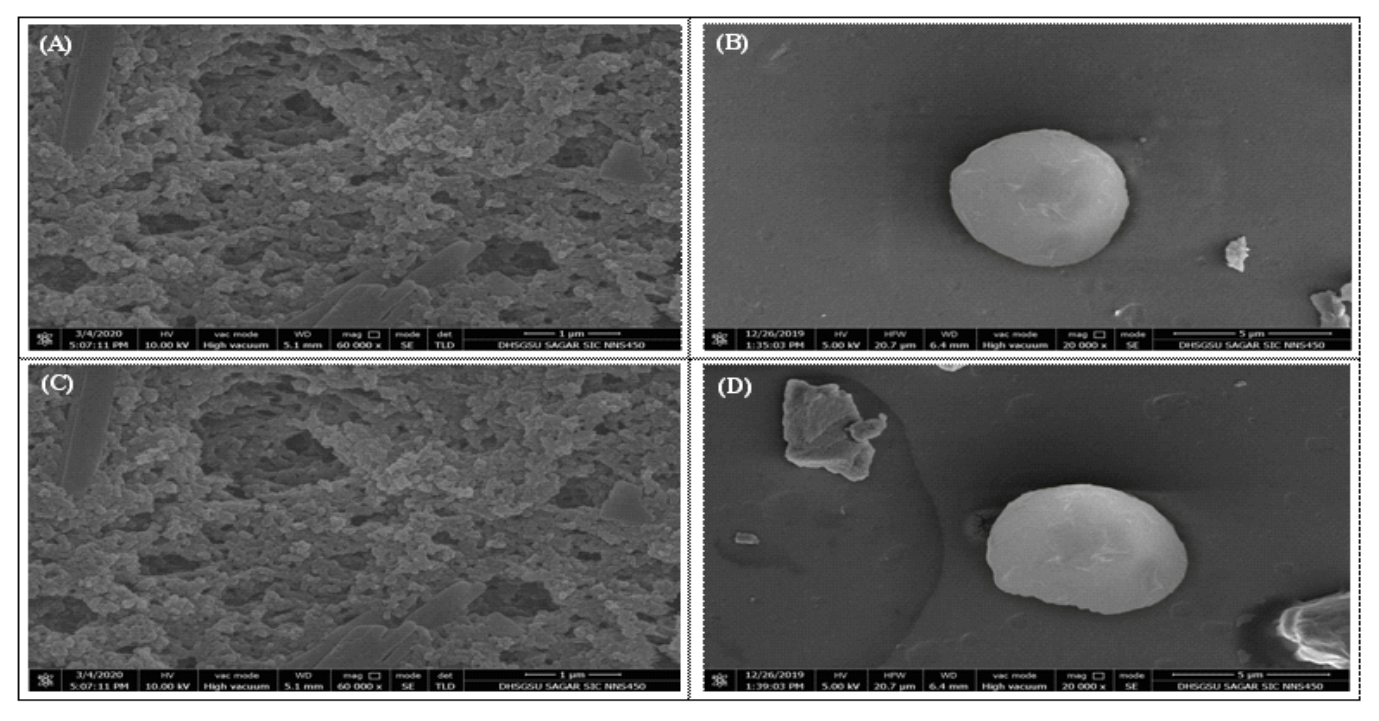


Figure 15. SEM photomicrographs of microspheres

### Percentage Entrapment efficiency (%EE)

The %EE of the folic acid conjugated paclitaxel loaded microspheres was determined using the method described by Wang et al., 2016 (Wang et al., 2016). The %EE of the paclitaxel-loaded liposomal formulation was found to be 85.00±0.5 % which is due to the passive loading of the drug (Table 12).

**Table 12.** % Entrapment efficiency of microspheres

S. No	Formulation code	% Entrapment efficiency
1	P2S2R3S3	85.00±0.5

### In vitro drug release

In vitro drug release studies of folic acid conjugated paclitaxel loaded microspheres were determined using a dialysis bag (molecular cut-off point 3,500) method at pH 6.8 and pH7. 4 (at  $37 \pm 0.5^{\circ}$ C), as reported by Wei et al., 2013 (Wei et al., 2013). The results of this study showed that the release was more at pH 6.8 as compared to pH 7.4. The drug release for folic acid conjugated paclitaxel loaded microsphereswas found to be 77.2±1.9% (pH 6.8) and 60.3±2.2% (pH 7.4) at 72 hrs, respectively. The cumulative % release of Paclitaxel from formulations is depicted in **figure 16.** 

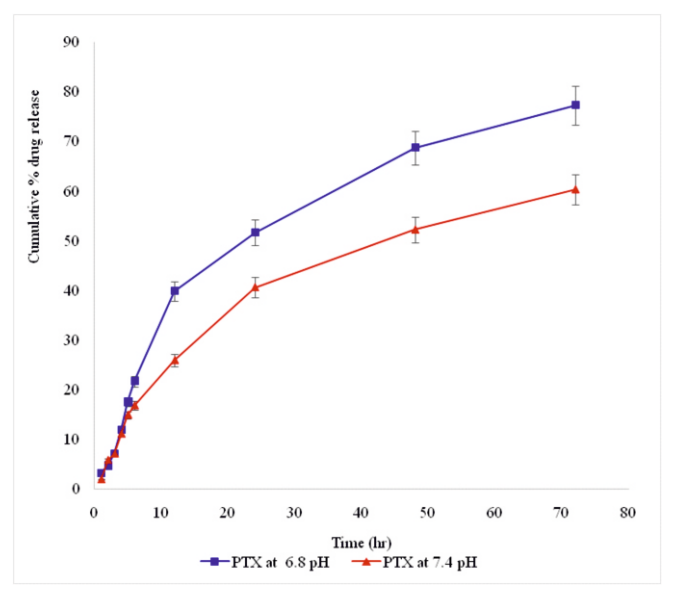


**Figure 16.** *In-vitro* drug release of FA-PTX microspheres in PBS pH 7.4 and PB 6.8

### Conclusion

In the realm of colorectal cancer treatment, folic acid conjugated microspheres have emerged as an innovative approach. This strategy leverages folic acid's specific binding to receptors that are often overexpressed on the surface of colorectal cancer cells. The present study has revealed several noteworthy findings. First and foremost, the synthesis of critical compounds, including the valine-paclitaxel conjugate and folic acid-paclitaxel (FA-PTX) conjugate, has demonstrated their potential to enhance the properties of

paclitaxel and enable its targeted delivery to cancer cells. Furthermore, the microspheres, prepared using the ionic gelation method, exhibit desirable characteristics. These include a uniform spherical morphology, which ensures stability, and an efficient drug loading process. This mechanism aims to maintain a consistent therapeutic drug level within the tumour, while simultaneously minimizing potential side effects.

In summary, these findings collectively suggest that folic acid-conjugated paclitaxel-loaded microspheres have the potential to be a valuable and effective treatment option for colorectal cancer. Their capacity for retention and penetration underscores their promise in cancer therapy. By combining the advantages of paclitaxel with targeted delivery through folic acid conjugation, this approach holds the potential to enhance treatment efficacy while reducing the side effects commonly associated with traditional chemotherapy for colorectal cancer. Nevertheless, to validate the practicality and fully unlock the potential of this innovative drug delivery system, further research, including *in vivo* studies and clinical trials, is warranted.

### Human and animal rights

No animals or humans were used in this study.

### Availability of data and material

The data will be available from the corresponding author, upon request.

### **Funding**

The writing of this article was not funded or supported by any specific grants or financial resources.

### **Conflict of interests**

The authors declare that they have no conflicts of interest.

# **Acknowledgements**

The authors are thankful to the Department of Pharmaceutical Sciences, Dr. Harisingh Gour Vishwavidyalaya (A Central University) Sagar for providing research resources and infrastructural facilities.

# References

Abu Samaan, T. M., Samec, M., Liskova, A., Kubatka, P., & Büsselberg, D. (2019). Paclitaxel's mechanistic and clinical effects on breast cancer. Biomolecules, 9(12), 789.

Biller, L. H., & Schrag, D. (2021). Diagnosis and treatment of metastatic colorectal cancer: a review. Jama, 325(7), 669-685.

Dozie-Nwachukwu, S., Danyuo, Y., Obayemi, J., Odusanya, O., Malatesta, K., & Soboyejo, W. (2017). Extraction and encapsulation of prodigiosin in chitosan microspheres for targeted drug delivery. Materials Science and Engineering: C, 71, 268-278.

Fan, R., Li, X., Deng, J., Gao, X., Zhou, L., Zheng, Y., Tong, A., Zhang, X., You, C., & Guo, G. (2016). Dual drug loaded biodegradable nanofibrous microsphere for improving anticolon cancer activity. Scientific reports, 6(1), 28373.

- Gohel, M., & Amin, A. F. (1998). Formulation optimization of controlled release diclofenac sodium microspheres using factorial design. Journal of Controlled Release, 51(2-3), 115-122.
- Hashiguchi, Y., Muro, K., Saito, Y., Ito, Y., Ajioka, Y., Hamaguchi, T., Hasegawa, K., Hotta, K., Ishida, H., & Ishiguro, M. (2020). Japanese Society for Cancer of the Colon and Rectum (JSCCR) guidelines 2019 for the treatment of colorectal cancer. International journal of clinical oncology, 25, 1-42.
- Ismail, S. T., Al-Kotaji, M. M., & Khayrallah, A. A. (2015). Formulation and evaluation of nystatin microparticles as a sustained release system. Iraqi Journal of Pharmaceutical Sciences (P-ISSN 1683-3597 E-ISSN 2521-3512), 24(2), 1-10.
- Kim, Y. J., & Kim, C. H. (2021). Treatment for peritoneal metastasis of patients with colorectal cancer. Annals of Coloproctology, 37(6), 425.
- Lv, C., Qu, H., Zhu, W., Xu, K., Xu, A., Jia, B., Qing, Y., Li, H., Wei, H.-J., & Zhao, H.-Y. (2017). Low-dose paclitaxel inhibits tumor cell growth by regulating glutaminolysis in colorectal carcinoma cells. Frontiers in Pharmacology, 8, 244.
- Moretto, R., Rossini, D., Zucchelli, G., Lonardi, S., Bergamo, F., Santini, D., Cupini, S., Tomasello, G., Caponnetto, S., & Zaniboni, A. (2020). Oligometastatic colorectal cancer: prognosis, role of locoregional treatments and impact of first-line chemotherapy—a pooled analysis of TRIBE and TRIBE2 studies by Gruppo Oncologico del Nord Ovest. European Journal of Cancer, 139, 81-89.
- Nars, M. S., & Kaneno, R. (2013). Immunomodulatory effects of low dose chemotherapy and perspectives of its combination with immunotherapy. International journal of cancer, 132(11), 2471-2478.
- Panda, P. K., & Jain, S. K. (2023). Polymeric Nanocarrier system Bearing Anticancer Agent for the Treatment of Prostate Cancer: Systematic Development and *in vitro* Characterization. International Journal of Pharmaceutical Investigation, 13(1).
- Rossi, S. M., Murray, T., McDonough, L., & Kelly, H. (2021). Loco-regional drug delivery in oncology: current clinical applications and future translational opportunities. Expert Opinion on Drug Delivery, 18(5), 607-623.

- Sharifi-Rad, J., Quispe, C., Patra, J. K., Singh, Y. D., Panda, M. K., Das, G., Adetunji, C. O., Michael, O. S., Sytar, O., & Polito, L. (2021). Paclitaxel: application in modern oncology and nanomedicine-based cancer therapy. Oxidative Medicine and Cellular Longevity, 2021.
- Siegel, R. L., Miller, K. D., Goding Sauer, A., Fedewa, S. A., Butterly, L. F., Anderson, J. C., Cercek, A., Smith, R. A., & Jemal, A. (2020). Colorectal cancer statistics, 2020. CA Cancer J Clin, 70(3), 145-164. https://doi.org/10.3322/caac.21601
- Tsai, M., Lu, Z., Wang, J., Yeh, T.-K., Wientjes, M. G., & Au, J. L.-S. (2007). Effects of carrier on disposition and antitumor activity of intraperitoneal paclitaxel. Pharmaceutical Research, 24, 1691-1701.
- Verma, A., Jain, A., Tiwari, A., Saraf, S., Panda, P. K., & Jain, S. K. (2021). Promising antifungal potential of engineered non-ionic surfactant-based vesicles: *in vitro* and *in vivo* studies. AAPS PharmSciTech, 22(1), 19.
- Wang, F., Yang, S., Hua, D., Yuan, J., Huang, C., & Gao, Q. (2016). A novel preparation method of paclitaxcel-loaded folate-modified chitosan microparticles and *in vitro* evaluation. Journal of Biomaterials Science, Polymer Edition, 27(3), 276-289.
- Wang, W., Xi, M., Duan, X., Wang, Y., & Kong, F. (2015). Delivery of baicalein and paclitaxel using self-assembled nanoparticles: synergistic antitumor effect *in vitro* and *in vivo*. International journal of nanomedicine, 3737-3750.
- Wei, H., Song, J., Li, H., Li, Y., Zhu, S., Zhou, X., Zhang, X., & Yang, L. (2013). Active loading liposomal irinotecan hydrochloride: Preparation, *in vitro* and *in vivo* evaluation. Asian Journal of Pharmaceutical Sciences, 8(5), 303-311.
- Xin, D., Wang, Y., & Xiang, J. (2010). The use of amino acid linkers in the conjugation of paclitaxel with hyaluronic acid as drug delivery system: synthesis, self-assembled property, drug release, and *in vitro* efficiency. Pharmaceutical Research, 27, 380-389.